Science Signaling
AAAS

www.sciencesignaling.org/cgi/content/full/11/530/eaao4617/DC1

Supplementary Materials for

IRE1α prevents hepatic steatosis by processing and promoting the degradation of select microRNAs

Jie-Mei Wang,* Yining Qiu, Zhao Yang, Hyunbae Kim, Qingwen Qian, Qinghua Sun, Chunbin Zhang, Lei Yin, Deyu Fang, Sung Hong Back, Randal J. Kaufman, Ling Yang,* Kezhong Zhang*

*Corresponding author. Email: kzhang@med.wayne.edu (K.Z.); jiemei.wang@wayne.edu (J.-M.W.); ling-yang@uiowa.edu (L.Y.)

Published 15 May 2018, *Sci. Signal.* **11**, eaao4617 (2018)
DOI: 10.1126/scisignal.aao4617

This PDF file includes:

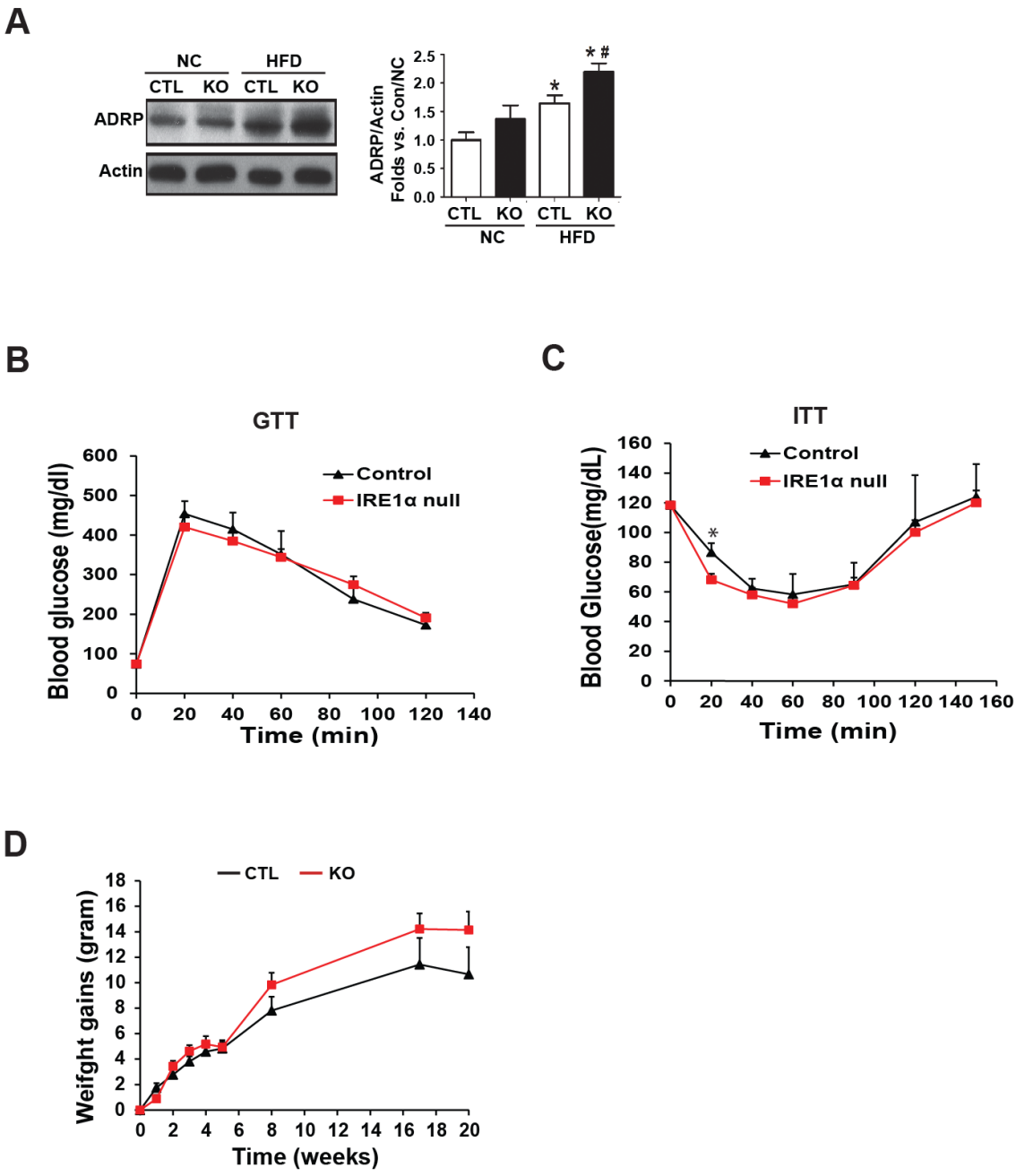

Fig S1. Metabolic phenotype of IRE1α-KO and control mice fed NC or an HFD. **(A)** Western blot analysis of ADRP protein levels in liver tissues from IRE1α KO and CTL mice fed with NC or a HFD for 20 weeks. The graph shows the quantification of ADRP protein levels in mouse livers. The ADRP protein signals, determined by Western blotting densitometry, were normalized to β-actin signals. Data are shown as mean ± SEM (n=4 mice per group). * $p<0.05$ vs. CTL + NC; # $p<0.05$ vs. CTL + HFD by unpaired 2-tailed Student's T-Test. **(B)** GTT analysis with the IRE1α KO and CTL mice under NC. The KO and CTL mice were fasted for 14 h and then intraperitoneally injected with 2mg glucose/gram body weight of glucose. Each point donates mean ± SEM (n=8 KO mice or 4 CTL mice). **(C)** ITT analysis with the KO and CTL mice under NC. The KO and CTL mice were fasted for 4 h and then intraperitoneally injected with 0.75mU/gram body weight of human insulin. Each point donates mean ± SEM (n=8 KO mice or 4 CTL mice). * $p<0.05$. **(D)** Body weight gains of the KO and CTL mice over 20 weeks of HFD. Each point donates mean ± SEM (n=8 KO mice or 4 CTL mice).

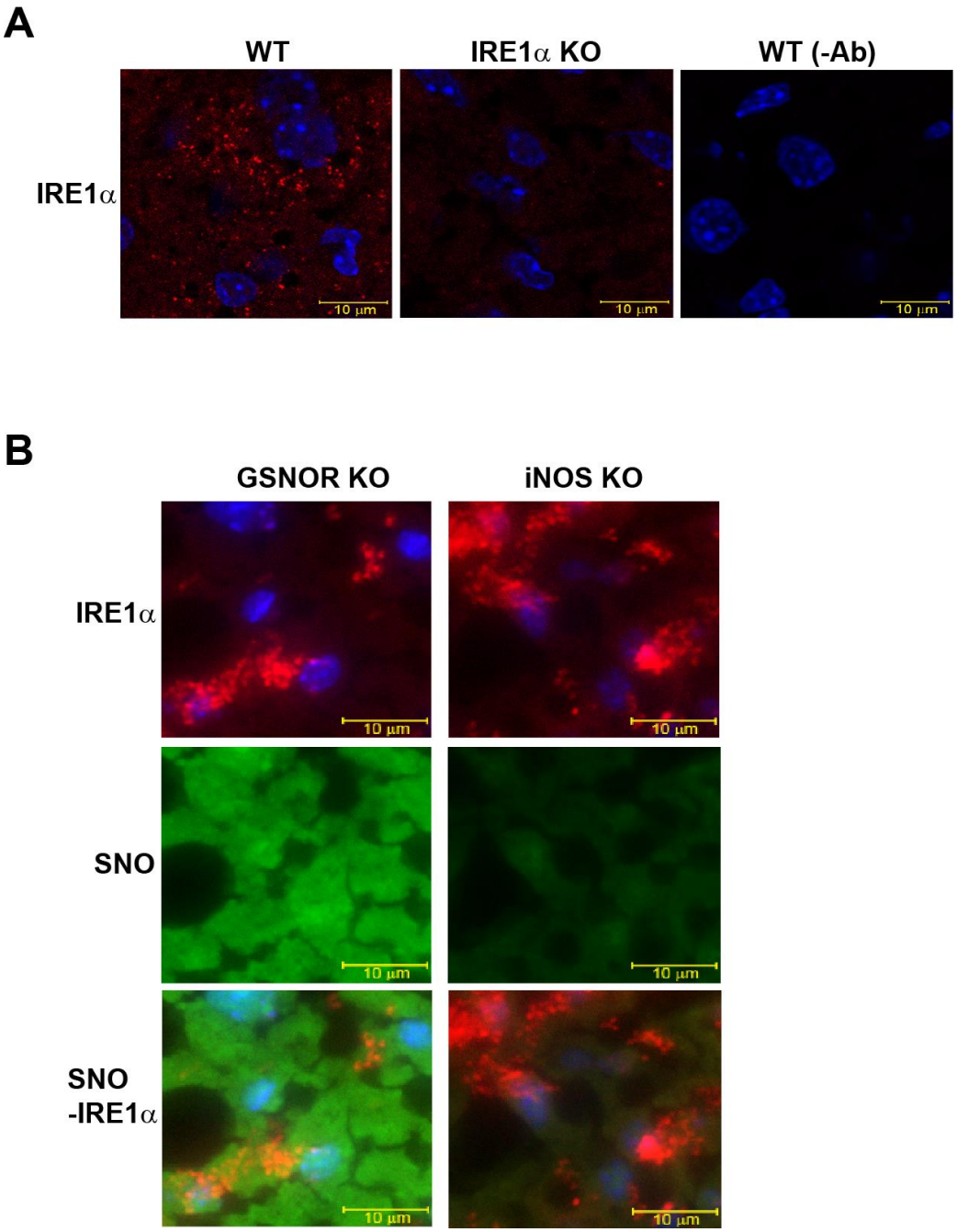

Fig S2. Immunofluorescent staining of IRE1α and S-nitrosylation signals in mouse liver tissues. (A) Representative images (63×) of staining for IRE1α in the livers of IRE1α KO and wild-type (WT) mice. Mouse liver tissue sections were subject to immunostaining for IRE1α using the anti-IRE1α antibody and the secondary antibody conjugated to Alex-568 (red fluorescence). Nucleus were stained with DAPI (blue). WT (-Ab) represent IRE1α antibody-omitted staining of the liver tissue sections of WT mice (negative/background control). Scale bar: 10μm. (**B**) Representative images (63×) of staining of SNO signals and IRE1α in liver tissues of S-Nitrosoglutathione Reductase (GSNOR)-KO or inducible nitric oxide synthase (iNOS)-KO mice under HFD. SNO proteins were visualized using Alexa-488 (green). Nucleus were stained with DAPI (blue). IRE1α immunostaining was performed in parallel using the anti-IRE1α antibody and the secondary antibody conjugated to Alex-568 (red). As a positive control for S-nitrosylation signals, immunofluorescent staining of the liver tissue sections of GSNOR KO mice under HFD showed extensive SNO protein signals in liver tissues, due to the defect of GSNOR. As a negative control for S-nitrosylation signals, immunohistochemistry staining of the liver tissue sections from iNOS-KO mice under HFD showed diminished protein SNO signals in liver tissues, due to the defect of iNOS. Scale bar: 10μm.

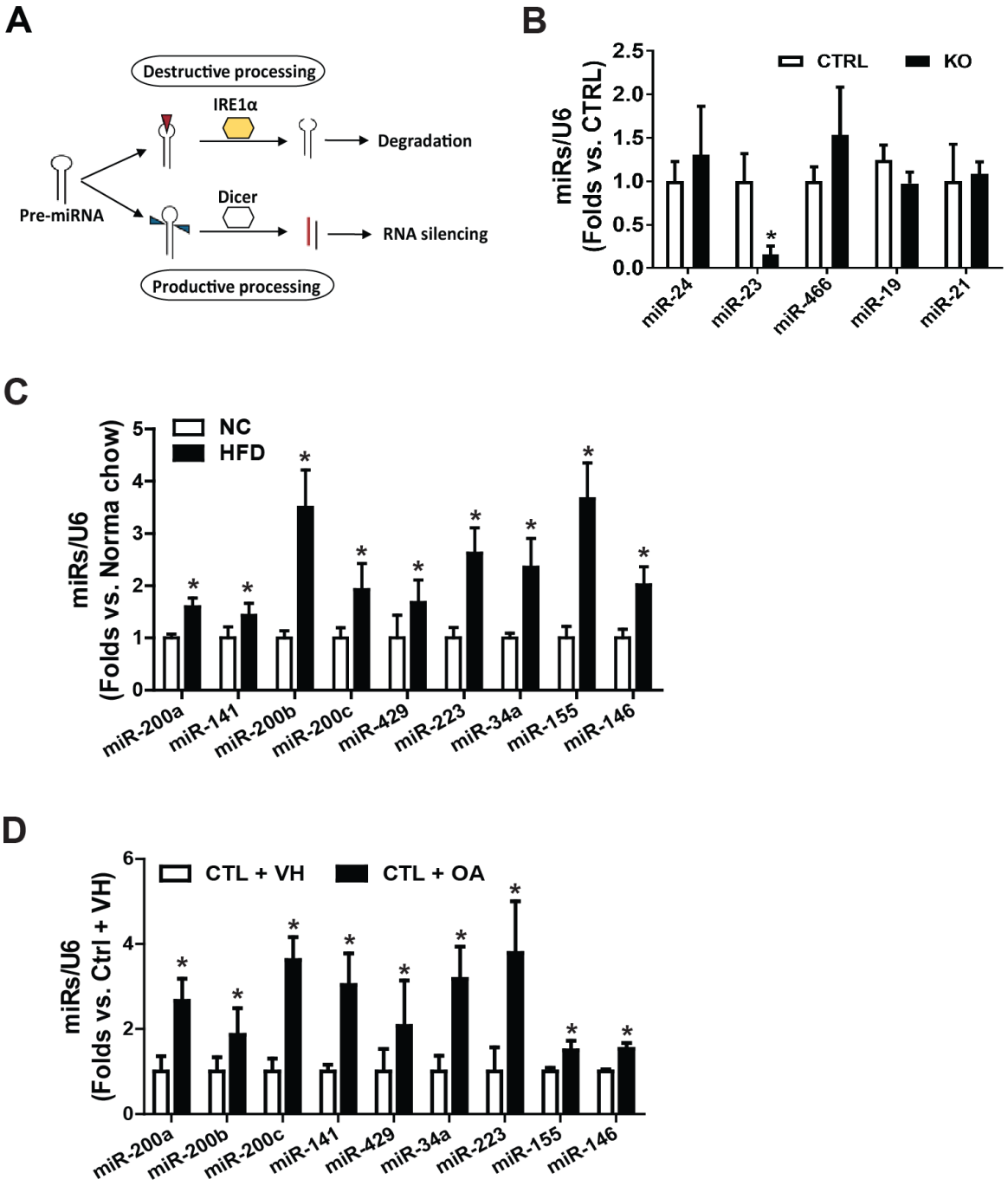

Fig S3. miRNA profiles in IRE1α-KO and control livers from NC- or HFD-fed mice and in OA-loaded mouse hepatocytes. (A) Illustration of IRE1α-mediated miRNA decay by processing pre-miRNA stem-loop structure. (**B**) miRNA-qPCR analyses of levels of the liver-enriched miRNAs, including miR-19, miR-21, miR-23, miR-24, and miR-466 in the livers of KO and CTL mice. The data are shown as means ± SEM (n=4 mice per group). * $p<0.05$ vs. CTL by unpaired 2-tailed Student's T-Test (B-D). (**C**) miRNA-qPCR analyses of levels of miRNA clusters in the livers of mice fed under NC or HFD diet for 20 weeks. The increases in all the miRNAs, as shown in the graph, were all statistically significant. * $p<0.05$ (n=4 mice per group). **(D)** miRNA-qPCR analysis of levels of miRNA clusters in mouse hepatocytes loaded with OA or 0.5% BSA vehicle (VH) for 24 h. The increases in all the miRNAs, as shown in the graph, were all statistically significant. The data are shown as means ± SEM (n=3 biological repeats). * $p<0.05$.

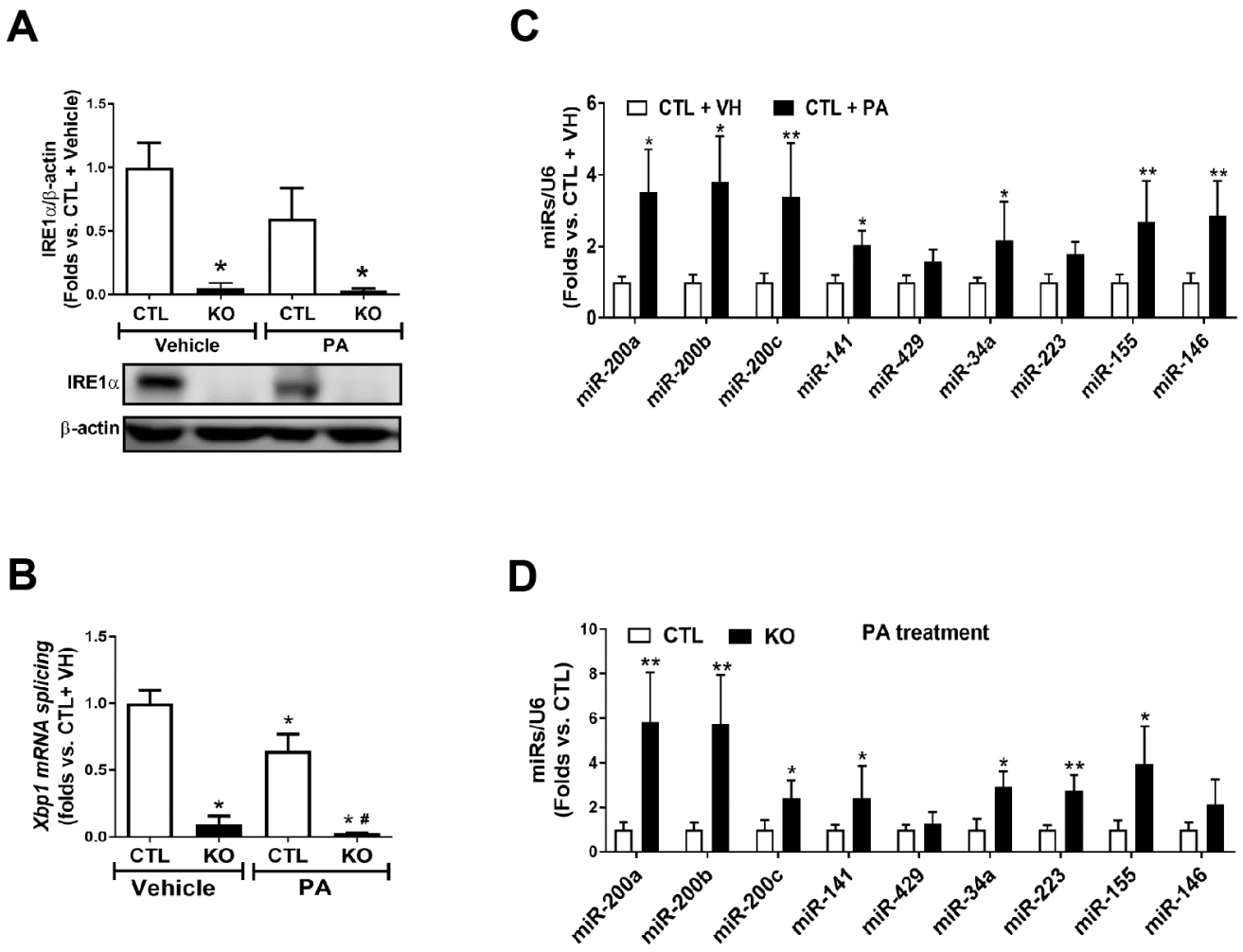

Fig S4. Palmitate represses IRE1α activity in processing select miRNAs. (**A**) IRE1α KO and CTL mouse hepatocytes were incubated with 5μM PA or 0.5% BSA vehicle for 36 h. Western blot analysis of IRE1α protein levels in IRE1α KO and CTL hepatocytes. The graph above is the quantification of IRE1α protein levels, determined by Western blotting densitometry, using β-actin as loading control. The data are shown as means ± SEM (n=3 biological repeats). * $p<0.05$. (**B**) qPCR analysis of the spliced *Xbp1* mRNA levels in IRE1α KO and CTL mouse hepatocytes under PA or vehicle as described in panel A. The data are shown as means ± SEM (n=3 biological repeats). * $p<0.05$. (**C**) miRNA-qPCR analysis of levels of miRNA clusters in mouse hepatocytes treated with 5 μM PA or vehicle for 36 h. The data was shown as mean ± SEM. * $p<0.05$ vs. CTL; ** $p<0.01$ vs. CTL (n=3 biological repeats). (**D**) miRNA-qPCR analysis of levels of miRNA clusters in IRE1α KO and CTL mouse hepatocytes treated with PA for 36 h. The data are shown as mean ± SEM. * $p<0.05$ vs. CTL; ** $p<0.01$ vs. CTL by unpaired 2-tailed Student's T-Test (n=3 biological repeats).

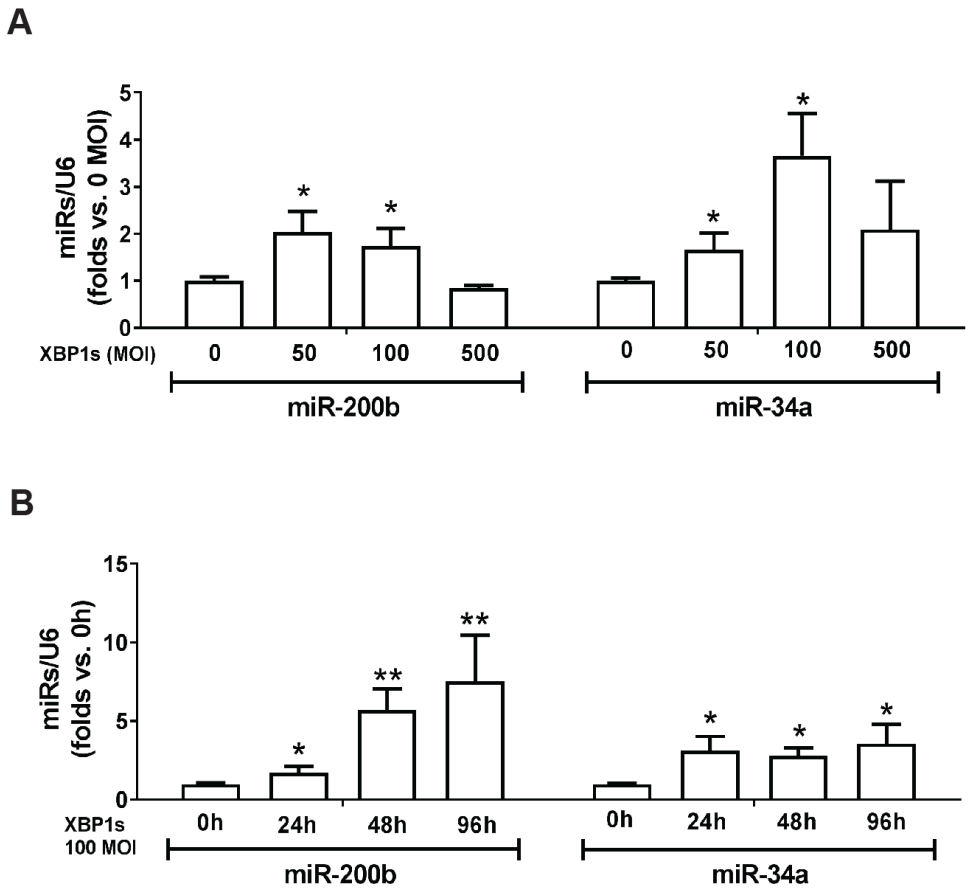

Fig S5. Titration and duration analyses for the effect of XBP1 overexpression on modulating miR-200 and miR-34. (**A**) Over-expression of the spliced/activated form of XBP1 (Ad-XBP1s) in wild-type mouse hepatocytes using adenoviral-based expression system at the doses of 0, 50, 100, and 500 MOI for 24 h. Mouse hepatocytes were injected with adenovirus expressing GFP (Ad-GFP) as a control (0 MOI). Levels of miR-200 and miR-34 family members, miR-200b and miR-34a, in the hepatocytes were determined by miRNA-qPCR analysis. The data are shown as means ± SEM (n=3 biological repeats per group). * $p<0.05$ vs. Control (0 MOI). (**B**) Wild-type mouse hepatocytes were infected with Ad-XBP1s at 100 MOI for 24, 48, and 96 h, using 0 h (samples collected immediately after the adenovirus was added) as control. Levels of miR-200b and miR-34a in the hepatocytes were determined by miRNA-qPCR analysis. The data are shown as means ± SEM (n=3 biological repeats per group). *$p<0.05$ vs. 0h, **$p<0.01$ vs. 0h by unpaired 2-tailed Student's T-Test.

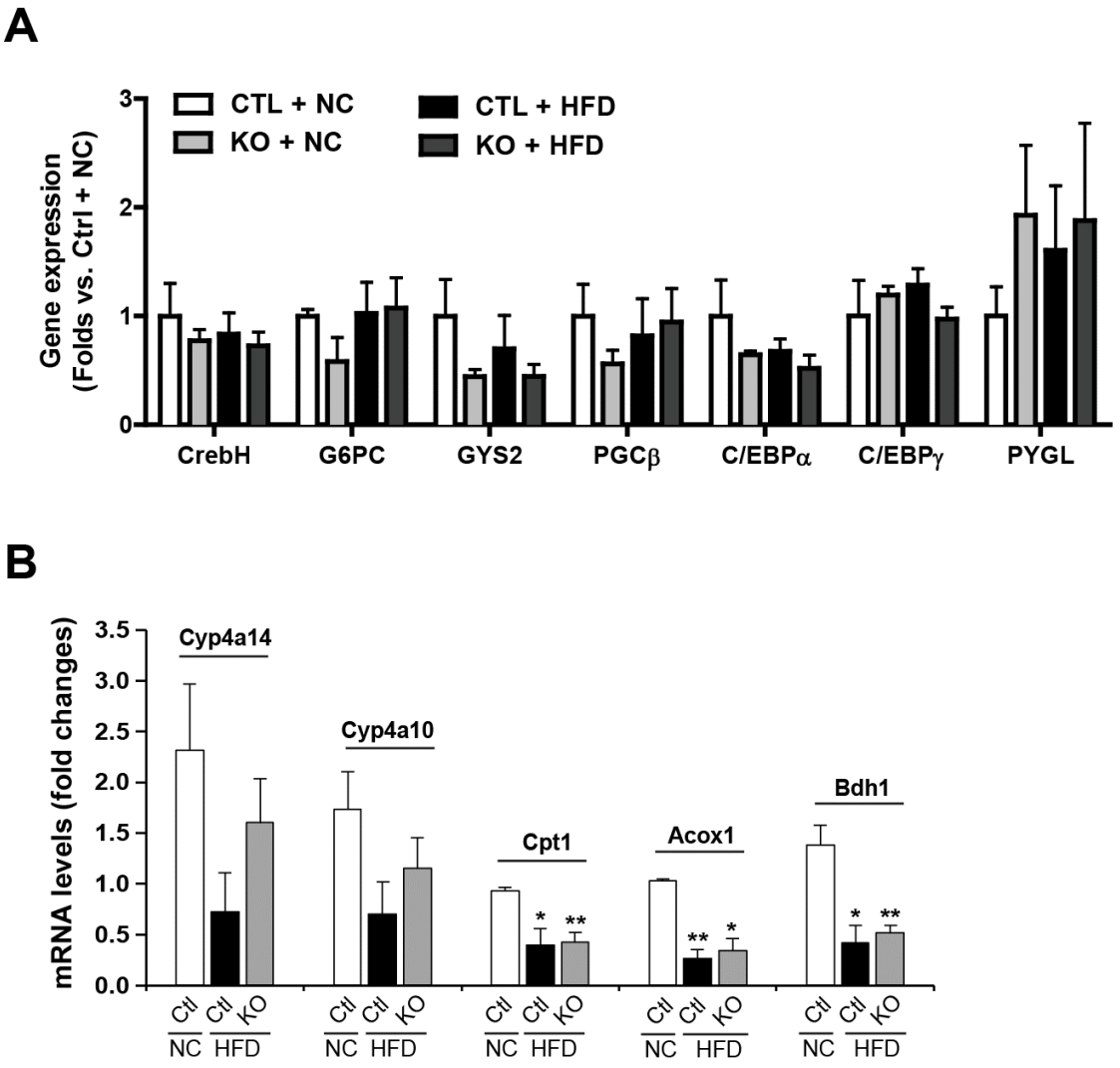

Fig S6. **Expression of the genes involved in lipid and glucose metabolism in IRE1α-KO and control mice fed NC or an HFD.** (**A**) qPCR analyses of expression levels of the mRNAs encoding key metabolic regulators in the livers of IRE1α KO and CTL mice fed with NC or HFD for 20 weeks. Data was shown as mean ± SEM (n=4 mice per group). (**B**) qPCR analyses of expression levels of the PPARα-target genes, including *Acox1*, *Cpt1*, *Cyp4a10*, and Cyp4a14, in the livers of IRE1α KO and CTL mice fed with NC or HFD. Data was shown as mean ± SEM (n=4 mice per group). * P<0.05; ** P<0.01 evaluated by unpaired 2-tailed Student's T-Test.

miR-200 and miR-34 binding sequences in the 3-UTR of *PPARα*

```
        3'  uguuGGUCGAUUCUGUGACGGu 5'  hsa-miR-34a
5065    5'  gcucCCAUCUCCUGGACUGCCa 3'  PPARA

        3'  uaccgucaccucaauCACUAAc 5'  hsa-miR-34b
 296    5'  cuuuagaucacauucGUGAUUu 3'  PPARA

        3'  cguuaGUCGAUUGAUGUGACGGa 5'  hsa-miR-34c-5p
5065    5'  gcucCCAUCU-CCUGGACUGCCa 3'  PPARA

        3'  ugUAGCAAUGGUCU-GUCACAAu 5'  hsa-miR-200a
7230    5'  ggAUUCUUUUGAAAUCAGUGUUa 3'  PPARA

        3'  aguaguaaugguccGUCAUAAu 5'  hsa-miR-200b
2408    5'  uggugcauccguuuCAGUAUUa 3'  PPARA

        3'  agGUAGUA-AUGGGC--CGUCAUAAu 5'  hsa-miR-200c
2404    5'  guCAUGGUGCAUCCGUUUCAGUAUUa 3'  PPARA

        3'  gguAGAAAUGGUCUGUCACAAu 5'  hsa-miR-141
7231    5'  gauUCUUUUGAAAUCAGUGUUa 3'  PPARA

        3'  ugccaaaauggucuGUCAUAAu 5'  hsa-miR-429
2408    5'  uggugcauccguuuCAGUAUUa 3'  PPARA
```

miR-200 and miR-34 binding sequences in the 3-UTR of *SIRT1*

```
        3'  uguUGGUCGAUUCUGUGACGGu 5'  hsa-miR-34a
877     5'  uccACAAG-UAUUAAACUGCCa 3'  SIRT1

        3'  cguuagucgauUGAUGUGACGGa 5'  hsa-miR-34c-5p
875     5'  uuuccacaaguAUUAAACUGCCa 3'  SIRT1

        3'  uguagcaAUGGUCU-GUCACAAu 5'  hsa-miR-200a
1713    5'  uuugaaaUACAAAACCAGUGUUu 3'  SIRT1

        3'  gguagaaAUGGUCU-GUCACAAu 5'  hsa-miR-141
1713    5'  uuugaaaUACAAAACCAGUGUUu 3'  SIRT1
```

Fig S7. miRNA-binding sequences of miR-200 and miR-34 family members in the 3′UTRs of human *PPARα* and *SIRT1* genes. Data are from microrna.org.

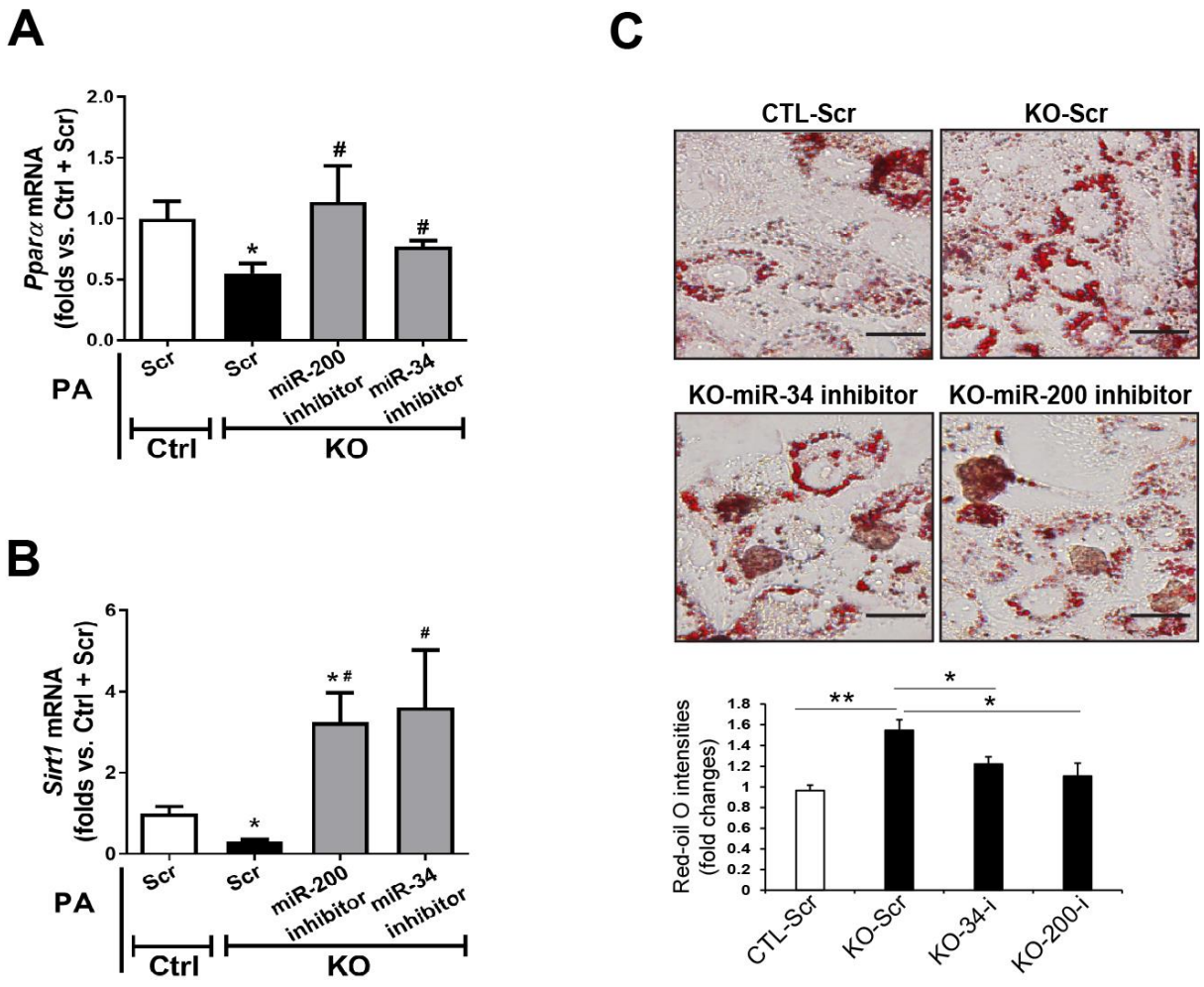

Fig S8. **Inhibition of miR-34 or miR-200 rescues *Pparα* and *Sirt1* expression and reduces hepatic steatosis caused by IRE1 deficiency and palmitate treatment.** (**A-B**) qPCR analyses of expression levels of *Pparα* (A) or *Sirt1* (B) mRNA in PA-treated IRE1α KO and CTL mouse hepatocytes transfected with scramble oligonucleotides (Scr), miR-34 antagomir (miR-34 inhibitor) or miR-200 family antagomir (miR-200 inhibitor). The data are shown as means ± SEM (n=3 biological repeats). * $p<0.05$ vs. CTL+Scr; # $p<0.05$ vs. KO+Scr by unpaired 2-tailed Student's T-Test. (**C**) Oil-red O staining of lipid droplet accumulation in the PA-incubated IRE1α KO hepatocytes that were treated with Scr, miR-34 inhibitor, or miR-200 inhibitor for 24 h. Scale bar: 10μm. The graph shows the quantification of lipids accumulated in the KO and CTL hepatocytes after the miR inhibitor or Scr treatment. Relative Oil Red O intensities were quantified using Image J software (NIH). 10 areas from each group were randomly selected for quantification. Data are shown as mean ± SD (n=10). * $p<0.05$; ** $p<0.01$.

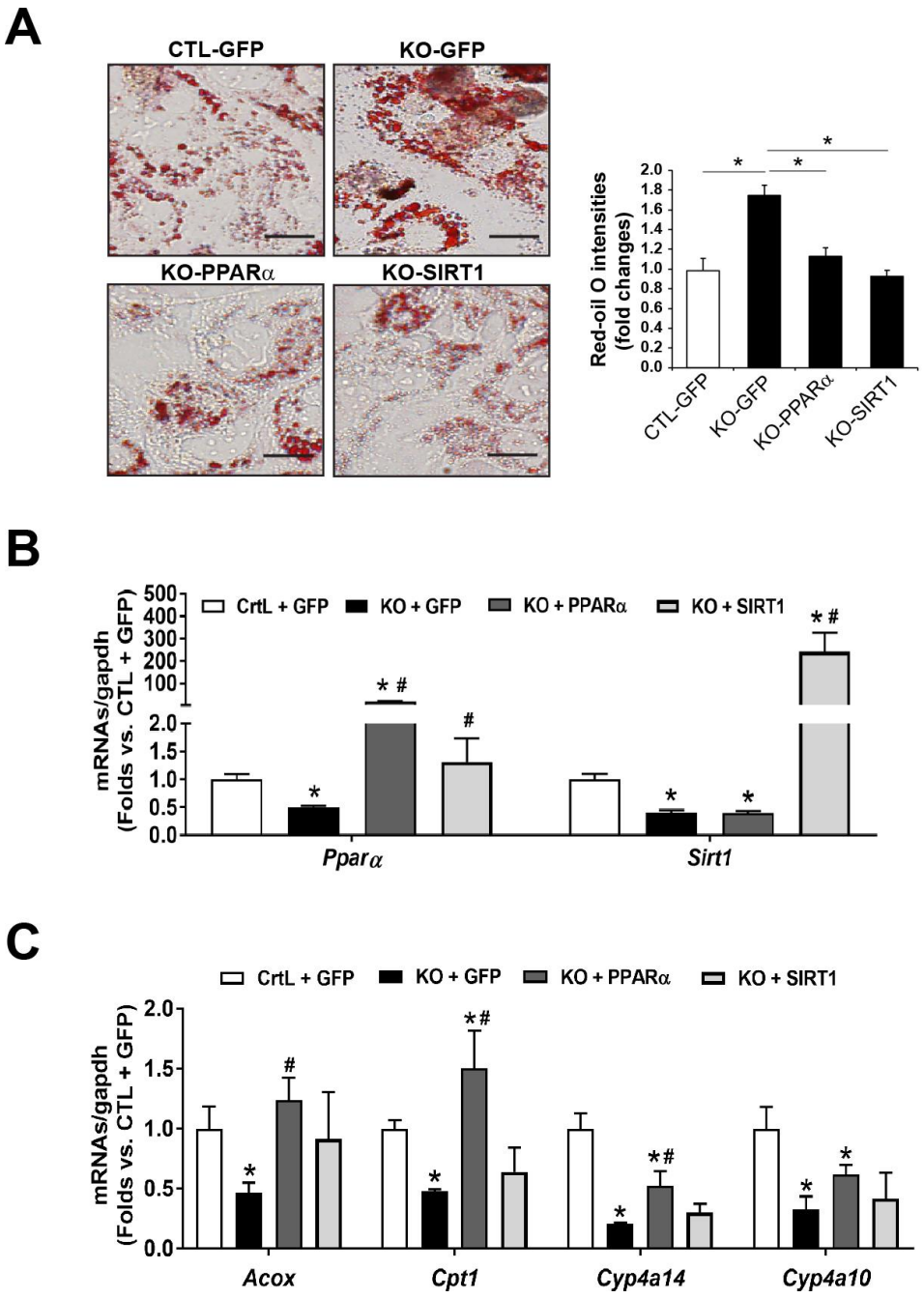

Fig S9. Overexpression of PPARα or SIRT1 reduces hepatic steatosis caused by IRE1 deficiency with palmitate treatment. (A) Oil-red O staining of neutral lipids in IRE1α KO hepatocytes over-expressing PPARα, SIRT1 or GFP, after incubation with PA (5μM) for 24 h. Scale bar: 10μm. The graph on the right side of the images shows the quantification of lipids accumulated in the KO and CTL hepatocytes. 10 areas from each group were randomly selected for quantification. Data are shown as mean ± SD (n=10). * p <0.05 determined by unpaired 2-tailed Student's T-Test. **(B-C)** qPCR analyses of expression levels of *Pparα* and *Sirt1* (B) as well as the PPARα target genes, including *Acox1*, *Cpt1*, *Cyp4a10*, and *Cyp4a14* (C), in PA-treated IRE1α KO and CTL mouse hepatocytes upon over-expression of GFP, PPARα, or SIRT1. Data are shown as mean ± SD (n=3 biological repeats). * p<0.05 vs. CTL+GFP. # p<0.05 vs. KO+GFP by unpaired 2-tailed Student's T-Test.

Liver-enriched miRs	Functional cluster	Published luciferase-validated targets	Selected literatures
miR-200 (miR-200a/b/c, miR-141, miR-429)	Liver injury, metabolism, pro-inflammatory,	HMGB1, ZEB1, ZEB2, PTEN, TKS5, MYLK.	*(42, 43, 51, 52)*
miR-34 (miR-34a/b/c)	Liver injury, metabolism, pro-inflammatory,	SIRT1, WNT1, ACSL1, NOTCH1, DLL1.	*(44, 53, 54)*
miR-155	Liver injury, metabolism, pro-inflammatory,	SHIP1, CASP-3, AICDA, ETS1, JARID2, SPI1, BACH1, FADD.	*(55, 56)*
miR-146	Pro-angiogenesis, anti-inflammatory, metabolism	IRAK1, TRAF6, WNT1/5a, CREB3L1, COX2.	*(44, 57, 58)*
miR-223	Liver injury, pro-inflammatory, pro-apoptotic	Rab1, NLRP3, ECT2, NFI-A, RhoB, STMN1.	(5*9, 60*)
miR-24	Anti-angiogenesis, Anti-inflammatory	CHI3L1, FGF11, MYC, E2F2, P16, PAK4.	(6*1, 62*)
miR-23	Pro-angiogenesis, pro-carcinogenic	E-cadherin, HIP1R, HES1, IL6R.	(6*3, 64*)
miR-19	Pro-inflammatory, Pro-carcinogenic	PTEN, Cullin 5, RUNX3, ATXN1.	(6*5, 66*)
miR-21	Liver injury, metabolism, anti-angiogenesis	ANP32A, BTG2, Bcl2, RECK, HNRPK, PPARγ, PTEN.	(6*7, 68*)
miR-466	Tumor suppressor, Anti-inflammation	Prox1, SGK1, RUNX2, IFN-α.	(6*9, 70*)

Table S1. miRNA functional clusters and previously identified targets. The table shows functional miRNAs (miRs) clusters that are enriched in the liver from healthy or patients with metabolic disorders or cancers, along with the function(s) and targets of each thus far identified. A selection of key studies are cited. All of the miRs listed have putative binding sites on 3'UTR of the *Pparα* and *Sirt1* genes except miR-24, based on the microrna database (microrna.org).